XII Stability and turning point bifurcations of a single particle in Poiseuille flow

Choi and Joseph 2001 performed simulations for single particle lift-off in Poiseuille flows at much higher shear Reynolds numbers. They observed that the rise and other equilibrium properties are not smooth functions of R. They found the existence of multiple steady states and hysteresis. Figure XII.1 shows the plot of h_e/d vs. R at different values of angular velocity of the particle. The particle density is 1.01 g/cc, W/d = 12, L/d = 22, η = 1 poise, d = 1 cm and ρ_f = 1 g/cc. The particle is initially placed close to the bottom wall. Simulations were performed in a periodic channel with three different conditions on the angular motion of the particle: zero hydrodynamic torque (free rotation), zero angular velocity (Ω_p = 0) and zero slip angular velocity (Ω_s = 0). In each of these cases the equilibrium height shows a sharp rise after a critical shear Reynolds number that is smallest for a non-rotating particle and is largest when the slip angular velocity is suppressed. The sharp rise or 'jump' in the equilibrium height can be explained in terms of turning point bifurcation to be discussed later. Choi & Joseph 2001 reported the freely rotating case shown in figure XII.1. The angular velocity of the particle is seen to have little effect on the equilibrium height before the 'jump.' The greater the slip angular velocity, the higher the particle rises after the 'jump.' Models for lift should account for this effect of the slip angular velocity.

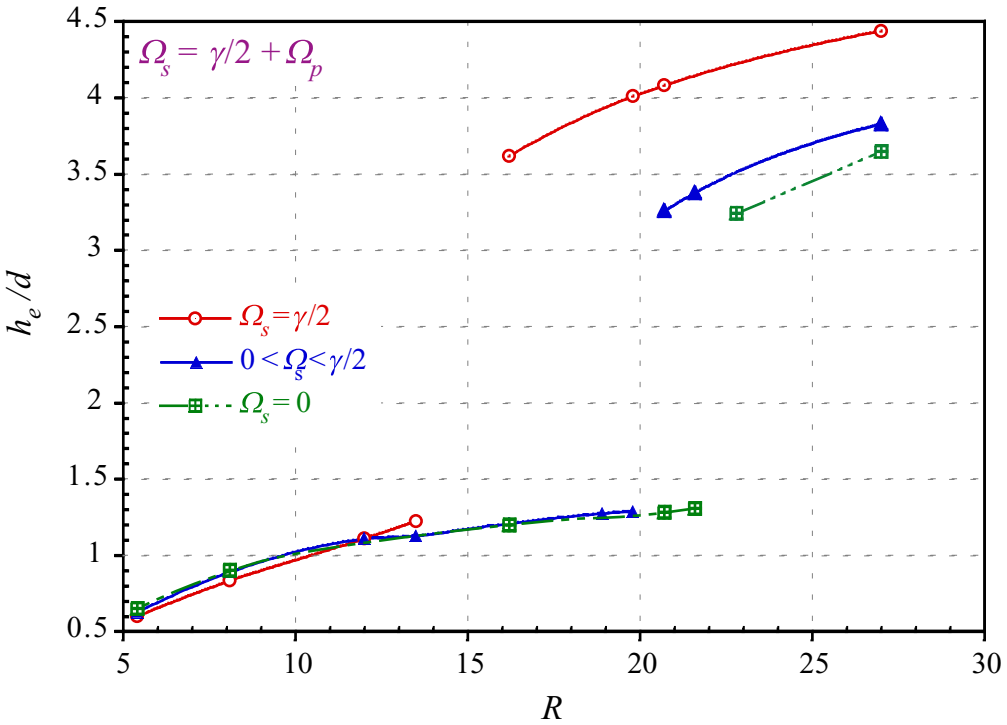

*Figure XII.1. Lift-off of a circular particle from a horizontal wall in a Poiseuille flow of a Newtonian fluid (*W/d = *12,* L/d = *22,* η = *1.0 poise,* d = *1 cm,* ρ_p = *1.01 g/cc).*

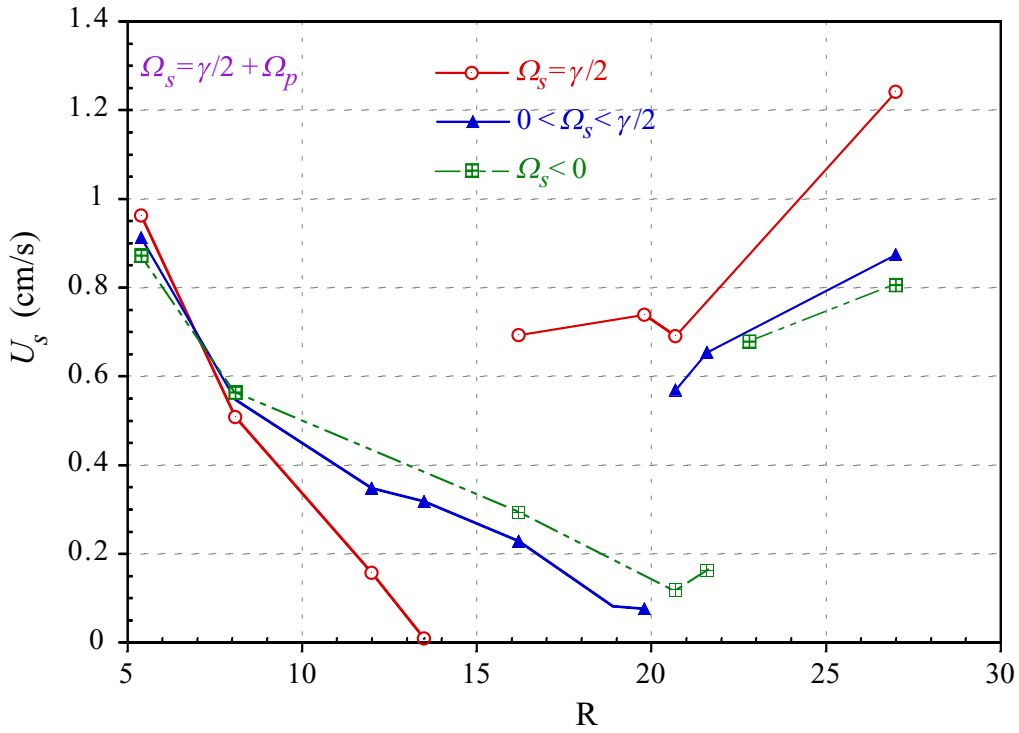

Figure XII.2. Slip velocity vs. shear Reynolds number for the cases depicted in figure XII.1.

Figure XII.2 shows the plot of slip velocity vs. R for the case above. It is seen that the slip velocity decreases before the 'jump' and increases sharply at the 'jump'. The slip velocity does not show a consistent trend with respect to the angular velocity of the particle. The slip angular velocity also shows a sharp change at the 'jump' (figure XII.3). As expected, the slip angular velocity is maximum for a non-rotating particle.

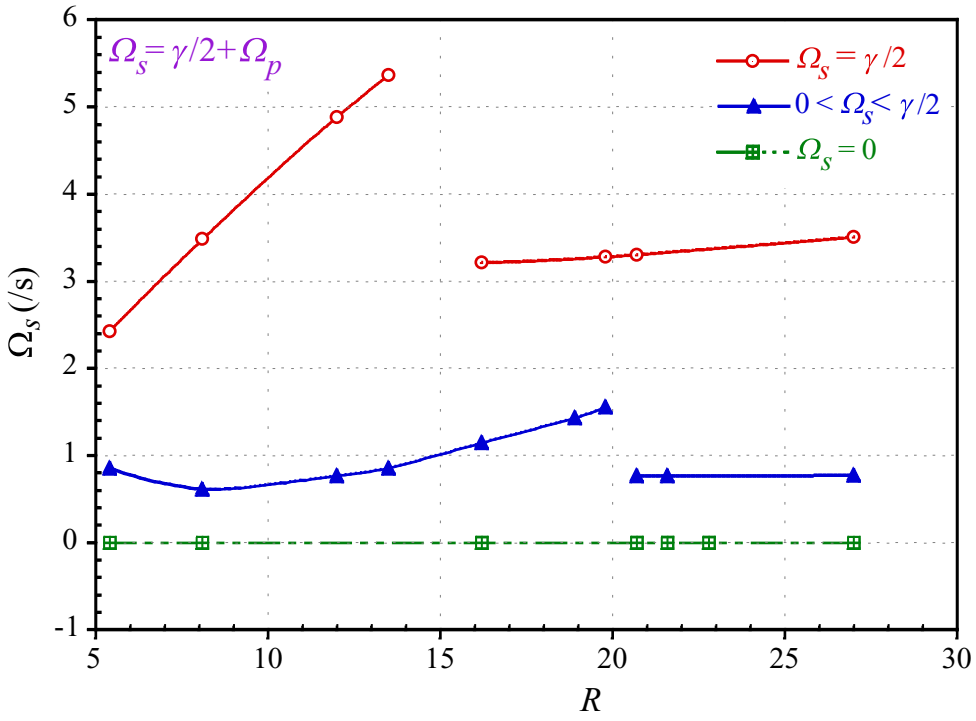

Figure XII.3. Slip angular velocity vs. shear Reynolds number for the cases depicted in figure XII.1.

In figure XII.4 we plot the rise of a neutrally buoyant particle to the equilibrium height as a function of time for W/d = 12, *L*/d = 22, d = 1 cm, η = 1 poise, ρ_f = 1 g/cc and R = 5.4. The simulations are performed in a periodic channel. We compare the rise of freely rotating and non-rotating particles. A neutrally buoyant freely rotating particle rises to a Segré-Silberberg radius; the non-rotating one rises more. A smaller lift is obtained when the slip angular velocity is entirely suppressed (Ω_s = 0) but the particle does rise. The greater the slip angular velocity the higher the particle rises.

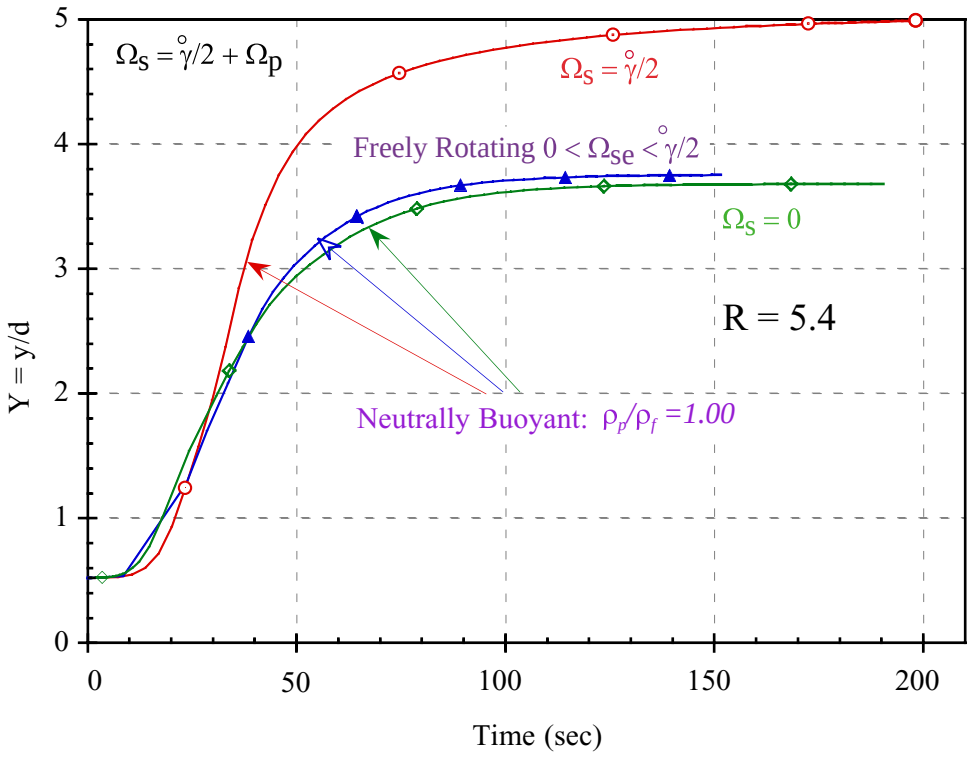

Figure XII.4. Rise vs. time for a neutrally buoyant particle (R = 5.4, W/d = 12, l/d = 22, η = 1 poise, d = 1 cm).

Table XII.1 gives data for the results presented in figures XII.1-4. In the next section we discuss the contribution to the hydrodynamic lift force from pressure and shear stress in a Newtonian fluid.

To analyze the instability manifested in the jumps in rise heights and particle velocities found by Choi and Joseph 2001 and shown in table XII.1 we may use another simulation method introduced by Patankar, Huang, Ko and Joseph 2001. The motion is simulated in a periodic channel in which the particle is free to rotate and translate in the axial (*x*-) direction. The height of the particle center from the bottom wall of the channel is fixed so that it does not translate in the transverse direction. There is no external body force in the axial direction and no external torque is applied. Gravity acts in the negative *y*-direction. The particle is initially at rest and eventually reaches a state of steady motion.

*Table XII.1. Data structure for a freely translating circular particle levitated by Poiseuille flow (*W/d = *12,* L/d = *22,* d = *1 cm,* ρ_f = *1 g/cc and* η = *1 poise). Bold numbers are for freely rotating particles. All the dimensional variables are given in CGS units.*

R/G	R_G	R	$\overline{p}$	h_e	U_p	U_f	U_s	Ω_p	Ω_f	Ω_s
2.9725	9.81	5.40	0.90	0.6020	2.1250	3.0877	0.9627	0.0000	2.4291	2.4291
6.6881	9.81	8.10	1.35	0.8366	5.7950	6.3040	0.5090	0.0000	3.4853	3.4853
14.679	9.81	12.00	2.00	1.1130	11.960	12.117	0.1572	0.0000	4.8870	4.8870
18.578	9.81	13.50	2.25	1.2260	14.870	14.860	0.0100	0.0000	5.3708	5.3708
26.752	9.81	16.20	2.70	3.6200	40.260	40.953	0.6930	0.0000	3.2130	3.2130
39.963	9.81	19.80	3.30	4.0120	52.140	52.879	0.7389	0.0000	3.2802	3.2802
43.679	9.81	20.70	3.45	4.0830	55.070	55.761	0.6908	0.0000	3.3068	3.3068
74.312	9.81	27.00	4.50	4.4410	74.290	75.531	1.2414	0.0000	3.5077	3.5077
2.9725	**9.81**	**5.40**	**0.90**	**0.6268**	**2.2960**	**3.2079**	**0.9119**	**1.5600**	**2.4180**	**0.8579**
6.6881	**9.81**	**8.10**	**1.35**	**0.8923**	**6.1420**	**6.6902**	**0.5482**	**2.8330**	**3.4477**	**0.6147**
14.679	**9.81**	**12.00**	**2.00**	**1.1100**	**11.740**	**12.088**	**0.3479**	**4.1220**	**4.8900**	**0.7680**
18.578	**9.81**	**13.50**	**2.25**	**1.1300**	**13.500**	**13.818**	**0.3185**	**4.6240**	**5.4787**	**0.8548**
26.752	**9.81**	**16.20**	**2.70**	**1.2110**	**17.410**	**17.638**	**0.2284**	**5.3200**	**6.4652**	**1.1452**
36.413	**9.81**	**18.90**	**3.15**	**1.2760**	**21.470**	**21.552**	**0.0820**	**6.0080**	**7.4403**	**1.4323**
39.963	**9.81**	**19.80**	**3.30**	**1.2900**	**22.720**	**22.796**	**0.0762**	**6.2140**	**7.7715**	**1.5575**
43.679	**9.81**	**20.70**	**3.45**	**3.2610**	**48.590**	**49.159**	**0.5688**	**3.9550**	**4.7248**	**0.7698**
47.560	**9.81**	**21.60**	**3.60**	**3.3800**	**51.790**	**52.444**	**0.6540**	**3.9490**	**4.7160**	**0.7670**
74.312	**9.81**	**27.00**	**4.50**	**3.8310**	**69.540**	**70.415**	**0.8747**	**4.1040**	**4.8803**	**0.7763**
2.9725	9.81	5.40	0.90	0.6511	2.4530	3.3252	0.8722	2.4070	2.4070	0.0000
6.6881	9.81	8.10	1.35	0.9047	6.2120	6.7756	0.5636	3.4390	3.4393	0.0000
26.752	9.81	16.20	2.70	1.1990	17.190	17.483	0.2930	6.4810	6.4814	0.0000
43.679	9.81	20.70	3.45	1.2830	23.600	23.719	0.1186	8.1360	8.1368	0.0000
47.560	9.81	21.60	3.60	1.3080	25.010	25.173	0.1632	8.4460	8.4456	0.0000
52.991	9.81	22.80	3.80	3.2440	53.290	53.968	0.6784	5.2370	5.2364	0.0000
74.312	9.81	27.00	4.50	3.6520	67.790	68.595	0.8054	5.2830	5.2830	0.0000
∞	0	5.4	0.90	4.9999	15.670	15.749	0.0800	0.0000	0.4500	0.4500
∞	**0**	**5.4**	**0.90**	**3.7530**	**13.780**	**13.928**	**0.1480**	**0.9580**	**1.0110**	**0.0530**
∞	0	5.4	0.90	3.6810	13.630	13.780	0.1500	1.0440	1.0440	0.0000

At steady state the particle translates in the axial direction at a constant velocity and rotates at a constant angular velocity. At the prescribed height, these velocities are such that there is no net hydrodynamic drag or torque. The flow field at steady state is independent of the particle density since the particle acceleration is zero. Only the axial and angular motion equations of the particle are solved in our simulations. The steady state translational and angular velocities as well as the hydrodynamic lift force are independent of the particle densities used in our simulations. This has been confirmed from our numerical results.

The hydrodynamic lift force L on the particle in the transverse direction depends on the height of the particle and the shear Reynolds number for a Newtonian suspending fluid and given channel and particle dimensions. We can select a particle of density ρ_p given by

$$\rho_p = \rho_f + \frac{L}{V_p g}, \tag{XII.1}$$

such that the lift just balances the buoyant weight.

Figure XII.5 shows the plot L as a function of the height of its center at different values of shear Reynolds number. The suspending fluid is Newtonian, L/d = 22, W/d = 12 and d = 1 cm. The fluid density is 1 g/cc and its viscosity is 1 poise. This plot can be used to find the equilibrium height of a particle of given density at different values of R.

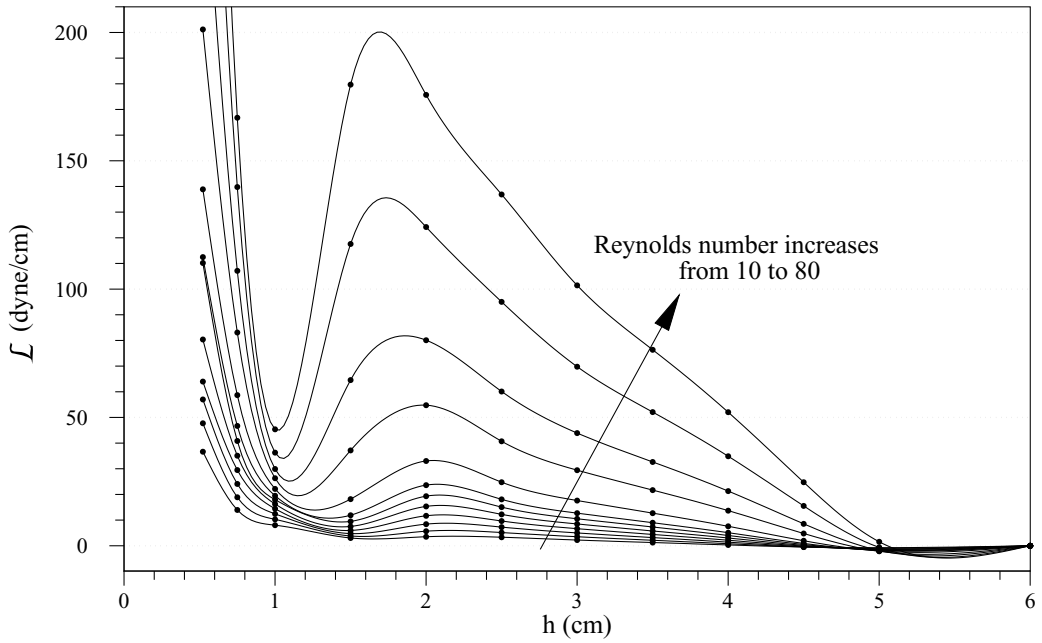

Figure XII.5. The hydrodynamic lift force on the particle as a function of the height of its center from the bottom wall at different shear Reynolds numbers. The bottom wall is h *= 0 cm and the channel centerline is* h *= 6 cm.*

A particle of density ρ_p will be in equilibrium at a height where $L = (\rho_p - \rho_f)gV_p$. As an example we consider a particle of density 1.01 g/cc. This particle will be in equilibrium when L = 7.705 dyne/cm. The equilibrium heights at a given shear Reynolds number are identified as the points of intersection between the curve of L vs. h and L = 7.705 in figure XII.6. The intersection points where the slope of the L vs. h curve is positive are unstable equilibrium points whereas a negative slope represents a stable equilibrium point (figure XII.6). Figure XII.7 shows the plot of equilibrium height of the particle of density 1.01 g/cc vs. R. We reproduce the bifurcation diagram given by Choi & Joseph 2001. They obtained this diagram by performing dynamic simulations where the particle was free to move in the transverse direction as well. Our results are in good agreement with theirs. In fact, we are also able to plot the unstable branch for the equilibrium height, which was not obtained from the dynamic simulations. From figure XII.7 we identify the nature of instability of the equilibrium height; it may be described as a double turning point bifurcation. The change of stability at a turning point is not really a bifurcation because a new branch of solutions does not arise at such a point (see, Iooss & Joseph 1990). The two turning points give rise to a hysteresis loop depicted in figure XII.7. Similarly, we can plot the equilibrium height diagrams for particles of different densities using figure XII.5.

Implications of multiple steady states for single particle lifting and on models of lift-off in slurries should be a subject of future investigation.

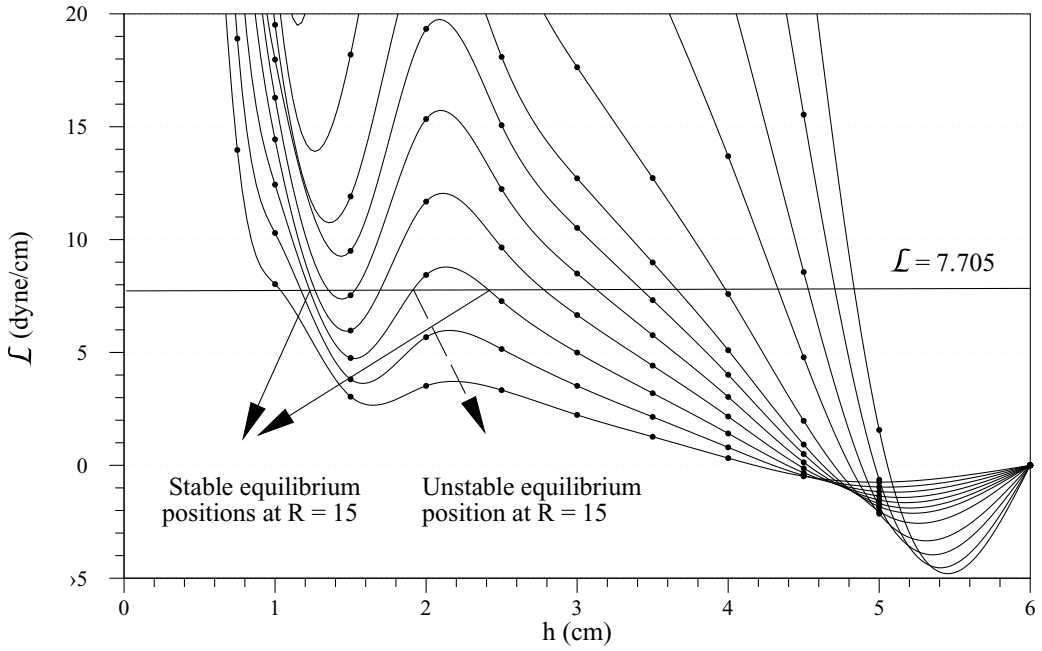

Figure XII.6. Finding the equilibrium height of a particle of a given density at different values of shear Reynolds number.

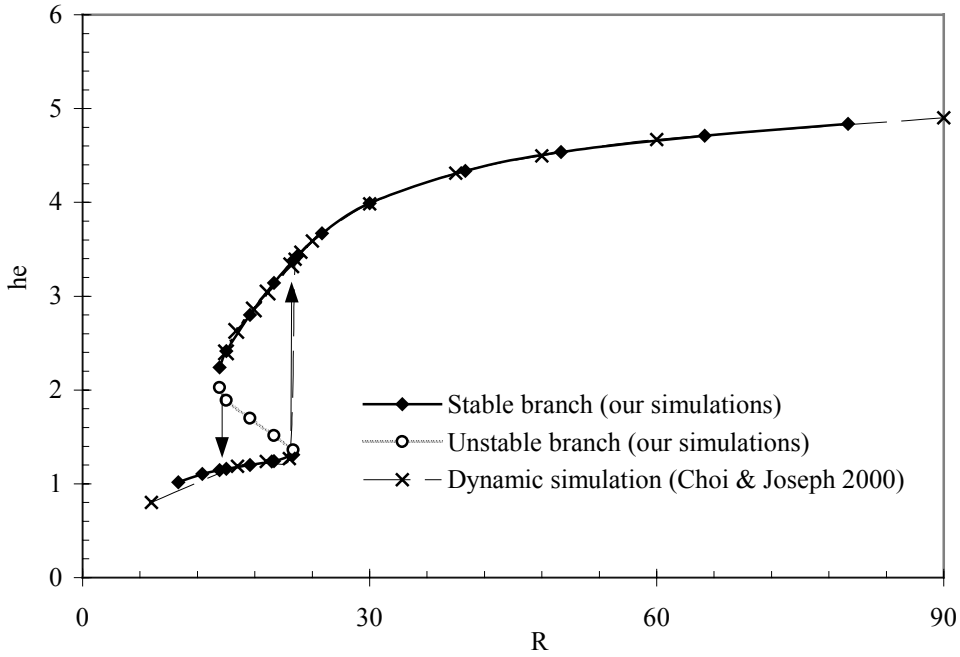

Figure XII.7. Equilibrium height as a function of shear Reynolds number for a particle of density 1.01 g/cm^3.

▪ Pressure lift and shear lift

Numerical simulation can be used to analyze the forces which enter into the lift balance

$$\begin{aligned} L_p + L_s &= \pi d^2 \left(\rho_p - \rho_f\right) g / 4, \\ L_p &= \oint_{\partial P} -p\mathbf{n}\, d\Gamma, \\ L_s &= \oint_{\partial \mathrm{P}} 2\eta \mathbf{D}[\mathbf{u}] \cdot \mathbf{n}\, d\Gamma, \end{aligned} \tag{XII.8}$$

where the buoyant weight is balanced by the sum of the pressure lift L_p and the shear lift L_s. It is well known that only the tangential (or shear) component of $2\eta\mathbf{D}[\mathbf{u}]\bullet\mathbf{n}$ is non-zero on a rigid surface. We define lift fractions

$$\begin{aligned} \Phi_p &= \frac{L_p}{L_p + L_s} \\ \Phi_s &= \frac{L_s}{L_p + L} \\ \Phi_p + \Phi_s &= 1 \end{aligned} \tag{XII.9}$$

In figure XII.8 we plot the lift fraction vs. R for cases shown in figure IX.4a; the figure shows that the pressure lift is greater than the shear lift and that the pressure lift fraction is greater for heavy particles. Figure XII.9 shows the plot of lift fraction vs. R for cases in figure XII.1. For a freely rotating particle the pressure lift is higher than the shear lift at lower shear Reynolds numbers but after the 'jump' they are of the same order. A non-rotating particle always has a greater contribution to lift from pressure.

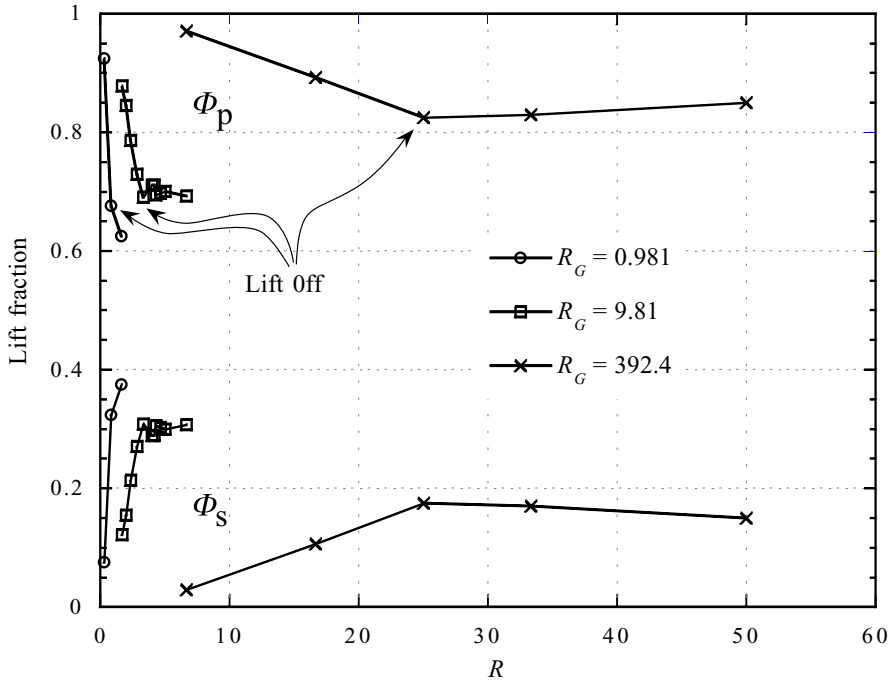

*Figure XII.8. Lift fractions due to the pressure and the viscous shear stress (*W/d *= 12). The pressure lift dominates.*

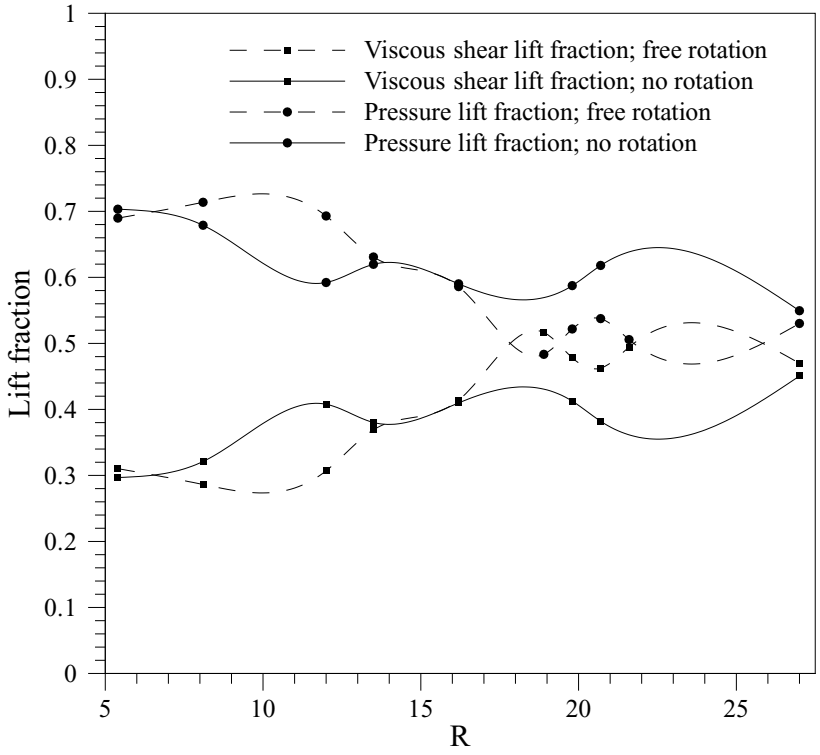

Figure XII.9. Lift fraction vs. shear Reynolds number for the cases shown in figure XII.1. Lift fractions for a freely rotating and a non-rotating particle are shown.

Figure XII.10 shows the pressure and the viscous shear stress distributions around the particle at different shear Reynolds numbers and particle rotations. The particle velocity lags the undisturbed fluid velocity (figure XII.11). The curvature of the undisturbed velocity profile creates a higher velocity of the fluid relative to the particle on the bottom half (figure XII.11). This was recognized by Feng, Hu and Joseph 1994b. The stronger relative flow on the bottom half results in a larger viscous shear stress at the bottom i.e. at $\theta = 180^o$ (figures XII.10a, b, e).

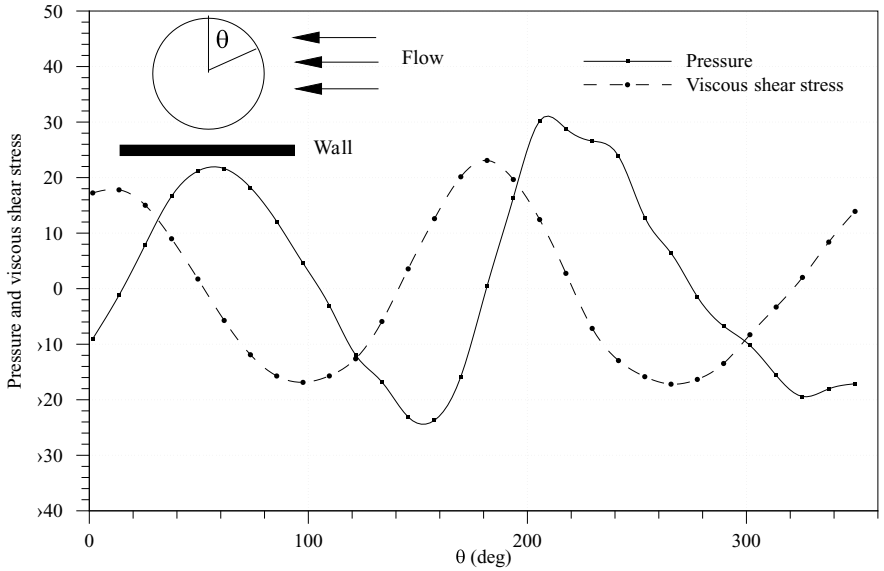

Figure XII.10(a). Distributions of pressure and viscous shear stress on the surface of a freely rotating circular particle in a Poiseuille flow of a Newtonian fluid. W/d = *12,* L/d = *22,* d = *1.0 cm,* ρ_p/ρ_f = *1.01,* R = *8.1 (before bifurcation).*

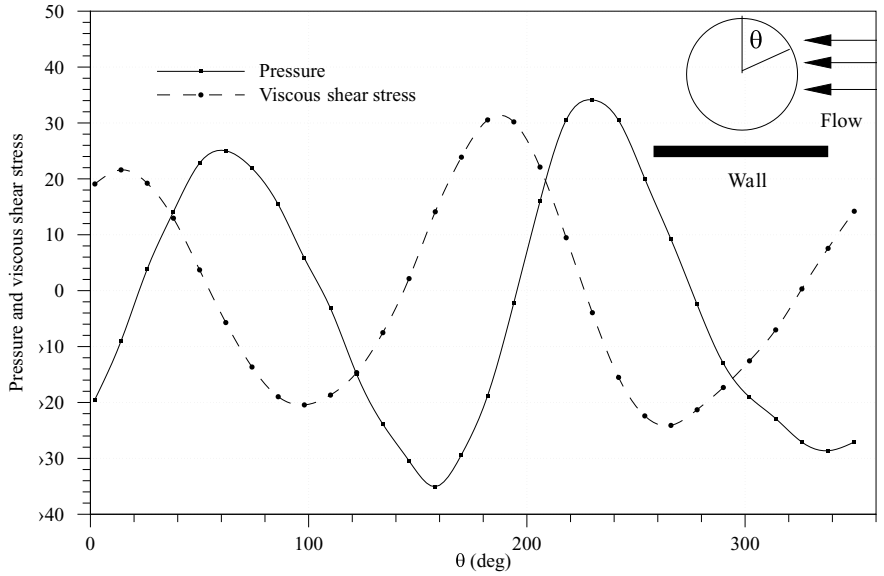

Figure XII.10(b). Distributions of pressure and viscous shear stress on the surface of a freely rotating circular particle in a Poiseuille flow of a Newtonian fluid. W/d = *12,* L/d = *22,* d = *1.0 cm,* ρ_p/ρ_f = *1.01,* R = *27 (after bifurcation).*

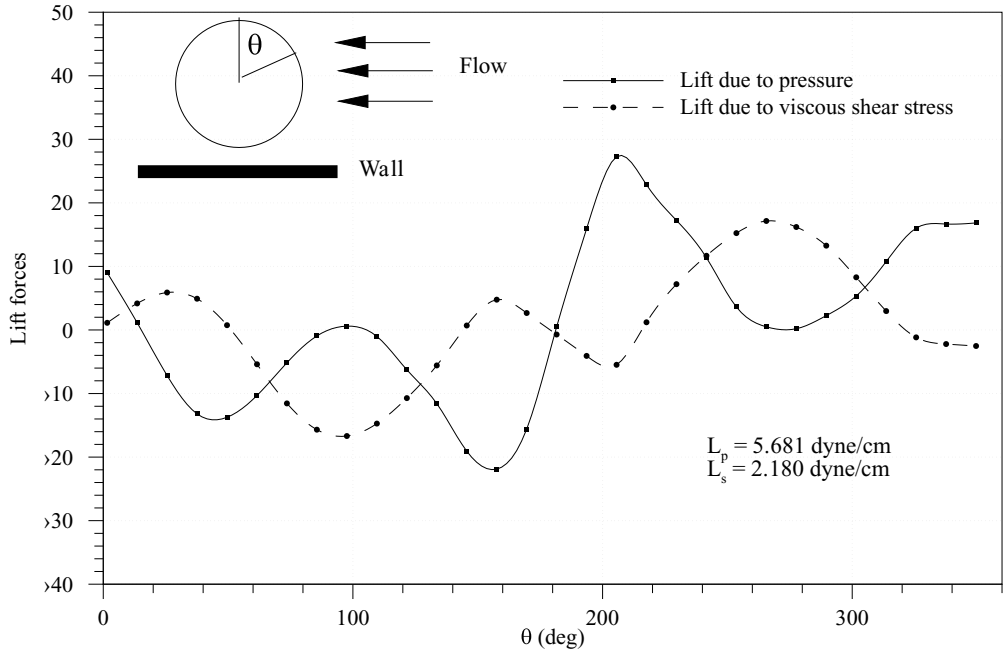

Figure XII.10(c). The distribution of lift forces on the surface of a freely rotating circular particle in a Poiseuille flow of a Newtonian fluid. W/d = *12,* L/d = *22,* d = *1.0 cm,* ρ_p/ρ_f = *1.01,* R = *8.1 (before bifurcation).*

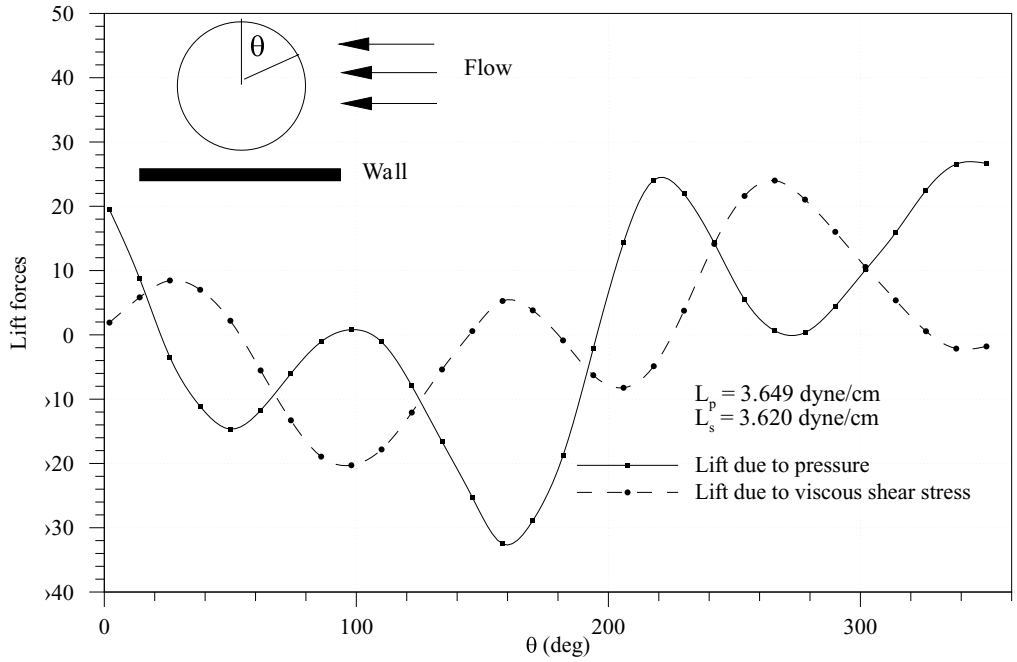

Figure XII.10(d). The distribution of lift forces on the surface of a freely rotating circular particle in a Poiseuille flow of a Newtonian fluid. W/d = *12,* L/d = *22,* d = *1.0 cm,* ρ_p/ρ_f = *1.01,* R = *27 (after bifurcation).*

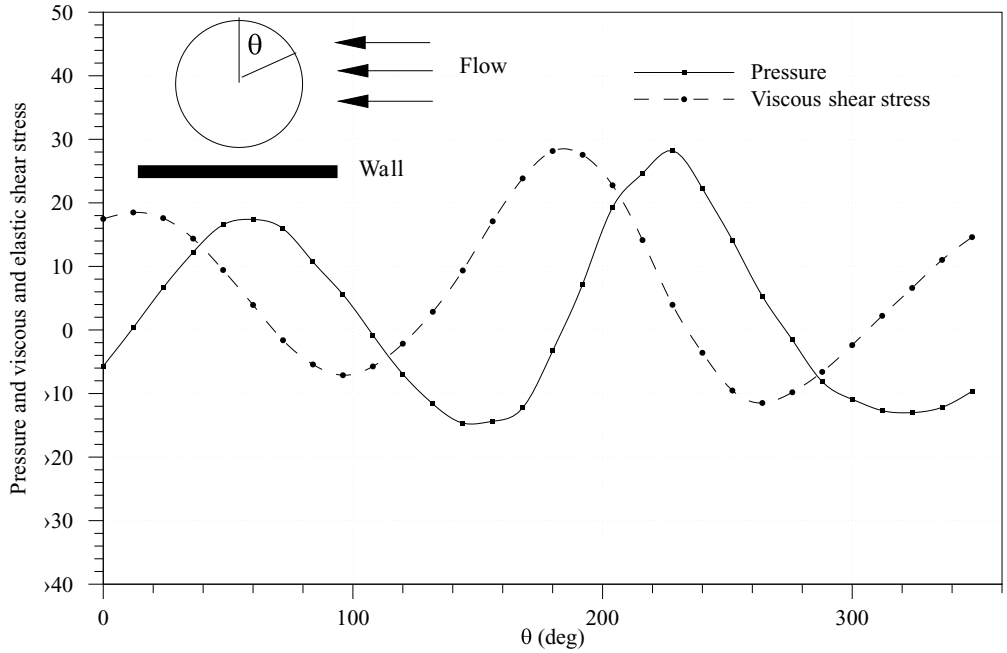

Figure XII.10(e). Distributions of pressure and viscous shear stress on the surface of a non-rotating circular particle in a Poiseuille flow of a Newtonian fluid. W/d = *12,* L/d = *22,* d = *1.0 cm,* ρ_p/ρ_f = *1.01,* R = *27 (after bifurcation).*

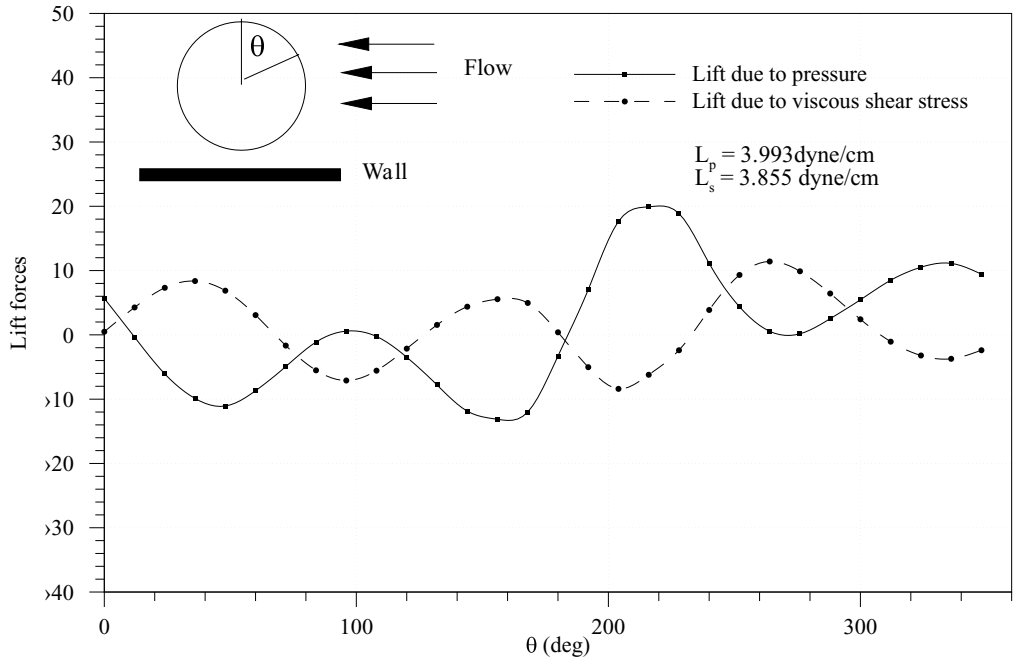

Figure XII.10(f). The distribution of lift forces on the surface of a non-rotating circular particle in a Poiseuille flow of a Newtonian fluid. W/d = *12,* L/d = *22*, d = *1.0 cm,* ρ_p/ρ_f = *1.01,* R = *27 (after bifurcation).*

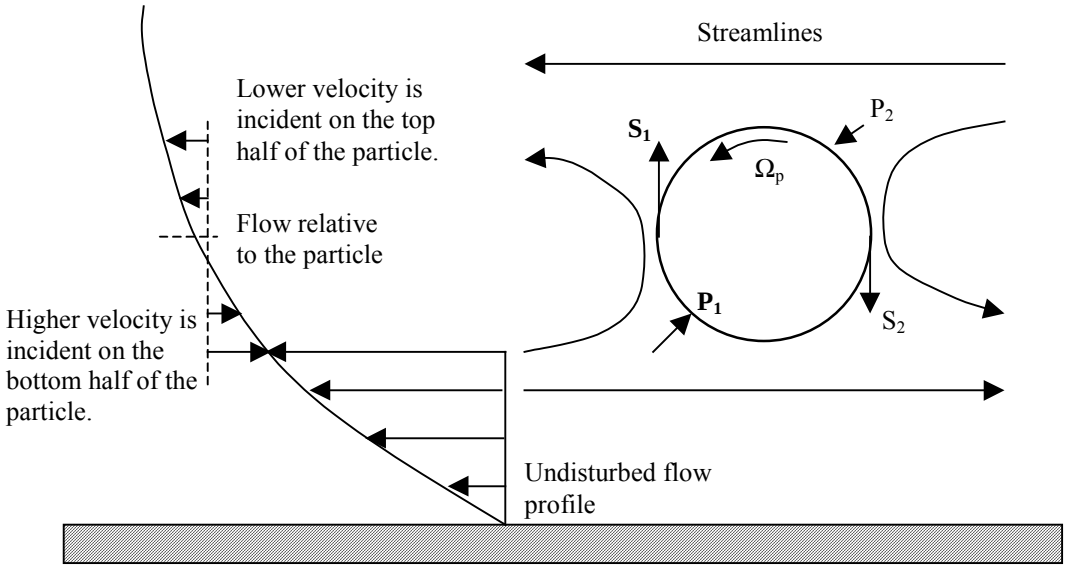

Figure XII.11. Cartoon depicting the fluid velocity and the streamlines relative to a particle in a plane Poiseuille flow. The fluid approaches the particle with higher velocity in the bottom half of the particle. Consequently, the pressure P_1 *(in bold) is greater than* P_2 *and the viscous shear stress* S_1 *(in bold) is greater than* S_2.

The analysis of the action of pressure and shear in levitating heavier than liquid particles may be carried out in the laboratory frame or in a frame fixed on the particle. In the laboratory frame we note that the forward motion of the particle pushes the fluid nearer the wall forward, inducing a return flow or vortex there. The high pressure on the bottom of the front face of the moving sphere near the stagnation point induces a high lift. This mechanism can also be described in the particle frame of reference.

Figure XII.11 shows the streamlines around the particle. The fluid velocity incident on the bottom half gives rise to the high pressure P_1 (in the third quadrant) that pushes the particle up. The incident fluid moves up, as shown by the streamline in figure XII.11, giving rise to the viscous shear stress S_1 at $\theta = 270^o$ in the upward direction. Similarly, pressure and shear forces, P_2 and S_2 respectively, act on the particle due to the velocity incident on the top half as shown in figure XII.11. Since the incident velocity on the bottom half is more, the lift due to P_1 and S_1 dominates giving rise to a net upward force on the particle. This is consistent with the observations in figures XII.10c, d and f. The regions of low pressure on the particle surface are seen to be less important in determining the lift on the particle as compared to the regions of high pressure.

The viscous shear stresses near $\theta = 90^o$ and $\theta = 270^o$ are smaller for a non-rotating particle. We see from figure XII.11 that the magnitudes of S_1 and S_2 would decrease for a non-rotating particle due to smaller relative velocities between the fluid and the particle surface at $\theta = 90^o$ and $\theta = 270^o$. The plot of viscous shear stress distribution is therefore shifted in the positive direction for a non-rotating particle (figure XII.10e) giving a greater lift as compared to a freely rotating particle at the same equilibrium height; a non-rotating particle is seen to rise more.

REMOVE THIS PAGE (only used to generate table of contents)